

## Unfolding and Refolding in Vitro of a Tetrameric, $\alpha$ -Helical Membrane Protein: The Prokaryotic Potassium Channel KcsA<sup>†</sup>

Francisco N. Barrera,<sup>‡</sup> M. Lourdes Renart,<sup>‡</sup> M. Luisa Molina,<sup>‡</sup> José A. Poveda,<sup>‡</sup> José A. Encinar,<sup>‡</sup> Asia M. Fernández,<sup>‡</sup> José L. Neira,<sup>‡,§</sup> and José M. González-Ros<sup>\*,‡</sup>

*Instituto de Biología Molecular y Celular, Universidad Miguel Hernández, Elche, 03202 Alicante, Spain, and Instituto de Biocomputación y Física de los Sistemas Complejos, 50009 Zaragoza, Spain*

*Received May 6, 2005; Revised Manuscript Received September 2, 2005*

**ABSTRACT:** 2,2,2-Trifluoroethanol (TFE) effectively destabilizes the otherwise highly stable tetrameric structure of the potassium channel KcsA, a predominantly  $\alpha$ -helical membrane protein [Valiyaveetil, F. I., Zhou, Y., and MacKinnon, R. (2002) *Biochemistry* 41, 10771–10777]. Here, we report that the effects on the protein structure of increasing concentrations of TFE in detergent solution include two successive protein concentration-dependent, cooperative transitions. In the first of such transitions, occurring at lower TFE concentrations, the tetrameric KcsA simultaneously increases the exposure of tryptophan residues to the solvent, partly loses its secondary structure, and dissociates into its constituent subunits. Under these conditions, simple dilution of the TFE permits a highly efficient refolding and tetramerization of the protein in the detergent solution. Moreover, following reconstitution into asolectin giant liposomes, the refolded protein exhibits nativelike potassium channel activity, as assessed by patch-clamp methods. Conversely, the second cooperative transition occurring at higher TFE concentrations results in the irreversible denaturation of the protein. These results are interpreted in terms of a protein and TFE concentration-dependent reversible equilibrium between the folded tetrameric protein and partly unfolded monomeric subunits, in which folding and oligomerization (or unfolding and dissociation in the other direction of the equilibrium process) are seemingly coupled processes. At higher TFE concentrations this is followed by the irreversible conversion of the unfolded monomers into a denatured protein form.

Knowledge on the mechanisms of “in vitro” folding of integral membrane proteins remains largely as an insufficiently documented subject (1–4). In this regard, two different groups of membrane proteins had been considered: those having a predominantly transmembrane  $\alpha$ -helical secondary structure, such as most receptor, channel, and transport proteins, and those characterized by membrane-spanning  $\beta$ -barrels, such as found in the outer membrane of bacteria. The predominantly  $\alpha$ -helical membrane proteins are more hydrophobic and quite resistant to chemical denaturation, and generally speaking, it is difficult to define solubilization conditions that allow denaturant removal and protein refolding (1–3). In these proteins, the so-called “two-stage model” remains as the basis to explain the folding process: individual  $\alpha$ -helices are formed first and then packed together inside the membrane to form a functional protein (5). On the other hand,  $\beta$ -barrel proteins are usually less hydrophobic, react somewhat similarly to soluble

proteins to classical denaturants, and are thought to have their own ways to fold and assemble into membranes (4).

The first membrane protein to be refolded in vitro from a fully unfolded state was bacteriorhodopsin, a proton pump from the purple membrane of archaeobacteria consisting of seven transmembrane  $\alpha$ -helices contained in a single polypeptide chain (6, 7). Regardless of the complexity of solubilization and refolding conditions, yields as high as 80–100% for refolding of bacteriorhodopsin had been reported, as well as recovery of retinal binding and proton pumping activity (reviewed in ref 2). Nevertheless and despite the obvious interest in bacteriorhodopsin and similar  $\alpha$ -helical monomeric proteins, the major challenge here is posed by the oligomeric membrane proteins, such as most receptors and channels present in eukaryotes, in which the information on their folding and assembly is almost nonexistent. Indeed, the bacterial diacylglycerol kinase (DAGK)<sup>1</sup> might be the sole reported example of in vitro refolding of such an oligomeric,  $\alpha$ -helical family of proteins (8, 9). Unfortunately, a high-resolution structure is still unavailable for DAGK, and its trimeric state is only supported by low-efficiency, cross-linking experiments. In fact, dissociation of the putative

<sup>†</sup> This work was supported by grants from the Spanish DGI BFI2002-03410 (to J.M.G.-R.) and CTQ2004-04474 (to J.L.N.) and from the Agencia Valenciana de Ciencia y Tecnología 03/056 (to J.M.G.-R.) and 04/B402 (to J.L.N.). F.N.B. and M.L.R. were partly supported by predoctoral fellowships from the Ministerio de Educación y Ciencia of Spain, while M.L.M. had a predoctoral fellowship from the Generalitat Valenciana.

\* To whom correspondence should be addressed. Tel: 34 96 665 8757. Fax: 34 96 665 8758. E-mail: gonzalez.ros@umh.es.

<sup>‡</sup> Instituto de Biología Molecular y Celular, Universidad Miguel Hernández.

<sup>§</sup> Instituto de Biocomputación y Física de los Sistemas Complejos.

<sup>1</sup> Abbreviations: KcsA, potassium channel from *Streptomyces lividans*; DDM, dodecyl  $\beta$ -D-maltoside; SDS-PAGE, polyacrylamide gel electrophoresis in the presence of sodium dodecyl sulfate; DAGK, bacterial diacylglycerol kinase; TFE, 2,2,2-trifluoroethanol; DPH, 1,6-diphenyl-1,3,5-hexatriene; CD, circular dichroism; FTIR, Fourier transform infrared spectroscopy; asolectin, a crude, commercial lipid extract from soybeans.

native trimer cannot be monitored during the unfolding of the protein, which led the authors to propose that trimer dissociation occurs at very low concentrations of the protein denaturant used in their studies (SDS; 8). Moreover, there is a high rate of misfolding during refolding from the SDS-unfolded state, which is interpreted as a specific feature of this particular protein (9).

In 1995, a relatively simple member of the potassium channel superfamily, the so-called KcsA, was identified in *Streptomyces lividans* (10). The ease of heterologous expression of KcsA in *Escherichia coli*, its resistance to harsh experimental conditions, and its purification in large quantities allowed for its crystallization and structural determination using X-ray diffraction methods (11). KcsA is a homotetramer in which each subunit is made up of 160 amino acids defining two transmembrane  $\alpha$ -helical segments connected by a pore region that contains an additional short helix and an ion selectivity filter homologous to the more complex eukaryotic potassium channels. The transmembrane segment M2, nearest to the C-terminus, contributes to the lining of the pore, while the one closest to the N-terminus, M1, is exposed to the membrane bilayer (11). Additionally, the N- and C-termini are included respectively in two relatively large cytoplasmic domains rich in charged or polar amino acid residues. These latter domains were not resolved in the crystal structure, which accounted only for the membrane-inserted 23–119 amino acids in the KcsA sequence (11). Nevertheless, electron spin resonance studies provided evidence that such domains form a fenestrated “hanging basket”-like structure underneath the membrane (12).

Thus, the existing structural information on KcsA, along with the availability of large quantities of the purified protein and the possibility of monitoring its biological function as a potassium channel upon reconstitution into lipid bilayers (10, 12–16), makes KcsA a potentially useful experimental system to undertake studies of folding in vitro of an oligomeric and predominantly  $\alpha$ -helical integral membrane protein. In this respect, however, the same intrinsic resistance of KcsA to harsh experimental conditions that facilitated some of the previous work on this protein makes folding studies somewhat difficult because the protein cannot be unfolded by conventional denaturants such as SDS (1 M), urea (7 M), guanidine hydrochloride (8 M), or guanidine isothiocyanate (5 M) (ref 17 and data not shown). Nevertheless, KcsA unfolding and dissociation into subunits can be attained in the presence of trifluoroethanol (TFE) or other short alcohols (17–19). In this paper, we are reporting on the TFE-induced unfolding and dissociation of KcsA and its in vitro refolding and tetramerization, which includes the recovery of its characteristic ion channel function.

## MATERIALS AND METHODS

**Protein Expression and Purification.** Expression of the wild-type KcsA protein with an added N-terminal hexahistidine tag in *E. coli* M15 (pRep4) cells and its purification by affinity chromatography on a Ni<sup>2+</sup>-NTA agarose column were carried out as reported previously (20) except that a higher dodecyl maltoside (DDM) concentration was present in the final buffer used with the purified protein (20 mM Hepes, pH 7.0, containing 100 mM KCl and 5 mM DDM). Also, a gel filtration step on a HiTrap desalting chromatog-

raphy column (Amersham Pharmacia Biotech) was employed to eliminate the imidazole used to elute the protein from the Ni<sup>2+</sup>-NTA agarose column. Protein concentration is always given in terms of KcsA monomers, using a molar extinction coefficient of 34950 M<sup>-1</sup> cm<sup>-1</sup>, as estimated from the extinction coefficients of model compounds (21).

1–125 KcsA was prepared by chymotrypsin hydrolysis of wild-type KcsA and characterized by MALDI tryptic peptide mass fingerprinting as described earlier (20), except that immobilized agarose-bound chymotrypsin (Sigma), at a protease to protein ratio of 15 units/mg of KcsA, was used in the experiments. The hydrolysis reaction was stopped by eliminating the agarose-bound protease by tabletop centrifugation. Cleaved fragments were also removed by a gel filtration chromatography step in Sephadex G-25.

**Fluorescence.** For this and all other experiments, the protein samples in detergent (DDM) solution were treated with TFE (Merck) at the desired concentrations by mixing the appropriate aliquots of stock protein and concentrated (10 $\times$ ) buffer solutions, distilled water, and TFE to a given final volume. Fluorescence measurements were taken on a SLM 8000 spectrofluorometer equipped with excitation and emission monochromators. The samples were contained in 0.5 cm path-length quartz cuvettes and thermostated using a Haake water bath. Excitation and emission wavelengths used in the different fluorescence measurements are given under the corresponding figure legends. Results are expressed in terms of the observed fluorescence intensity at a given wavelength or of the averaged emission intensity,  $\langle\lambda\rangle$ , as defined by

$$\langle\lambda\rangle = \sum_1^n (1/\lambda_i) I_i / \sum_1^n I_i$$

where  $I_i$  is the fluorescence intensity measured at a wavelength  $\lambda_i$  (22). The use of the  $\langle\lambda\rangle$  parameter (whose units are nm<sup>-1</sup>) is particularly suited to report on spectral shifts irrespective of any particular wavelength, as it integrates information from the fluorescence intensity emitted at all recorded wavelengths in the spectrum.

**Circular Dichroism.** Far-UV circular dichroism (CD) spectra were taken on a Jasco J810 spectropolarimeter at a 100 nm/min scan rate and using a 2 nm resolution. The samples were thermostated with a Jasco Peltier system and contained into 0.1 cm path-length quartz cuvettes. The molar ellipticity,  $[\Theta]$ , was calculated as

$$[\Theta] = \Theta/10lc(N - 1)$$

where  $\Theta$  is the measured ellipticity;  $l$ , the path length;  $c$ , the KcsA molar concentration in terms of KcsA monomers; and  $N$ , the number of amino acid residues.

**Fourier Transform Infrared Spectroscopy.** For infrared amide I' band recordings from KcsA samples, aliquots of KcsA in 20 mM Hepes, pH 7.0, containing 100 mM KCl and 5 mM DDM were washed twice with 2 mL of 1 mM Hepes, pH 7.0, 10 mM KCl, and 1 mM DDM, and its volume was reduced to about 200  $\mu$ L by filtration on Vivaspinn concentrators (5000 MW cutoff; Vivascience). The concentrated samples were then dehydrated in a Speed Vac Savant rotary evaporator and resuspended in 20  $\mu$ L of D<sub>2</sub>O (or D<sub>2</sub>O/TFE mixtures) to avoid the interference of H<sub>2</sub>O infrared

absorbance ( $1645\text{ cm}^{-1}$ ). The resulting solutions were placed into a liquid demountable cell equipped with  $\text{CaF}_2$  windows and  $50\text{ }\mu\text{m}$ -thick Mylar spacers and maintained at room temperature for approximately 40 min to reach equilibrium. The final KcsA concentration in the cell was approximately  $0.65\text{ mM}$ . Infrared spectra were taken in triplicate (600 spectral scans each) in a Bruker IF66s instrument equipped with a DTGS detector. Buffer contribution was subtracted from the individual spectra, and spectral noise was reduced as described previously (23). The protein secondary structure was estimated by decomposing the amide I' band into its spectral components as reported earlier (24).

**SDS-PAGE.** Protein aliquots in the DDM-containing media were treated with TFE at different concentrations as indicated in the legend to Figure 5, then mixed with an equal volume of electrophoresis sample buffer (20 mM Tris, pH 6.8, 20% glycerol, 0.1% bromophenol blue, and 4% SDS), and run in 13.5% PAGE in the presence of 0.1% SDS (25). After Coomassie Brilliant Blue staining, the intensity of the bands was measured by densitometry.

**Analytical Ultracentrifugation.** Sedimentation velocity experiments were conducted in a Beckman Optima XL-I ultracentrifuge (Beckman Coulter) with an An50Ti eight-hole rotor and double-sector Epon-charcoal centerpieces. The samples were centrifuged at 50000 rpm,  $21\text{ }^\circ\text{C}$ , and the absorbance at 280 nm was followed. Differential sedimentation coefficient distributions,  $c(s)$ , were calculated by least-squares boundary modeling of sedimentation velocity data by using the program SEDFIT (26, 27). The results were corrected for the viscosity and density of the different TFE solutions used, to yield the  $s_{20,w}$  values.

**Electrophysiological Recordings.** For patch-clamp measurements of potassium channel activity, the refolded KcsA was first reconstituted in asolectin lipid vesicles, as reported previously (20). Giant liposomes ( $10\text{--}100\text{ }\mu\text{m}$ ) were then prepared by submitting a mixture of the reconstituted vesicles (containing  $50\text{ }\mu\text{g}$  of refolded protein) and asolectin vesicles ( $25\text{ mg}$  of total lipids) to a cycle of partial dehydration/rehydration (28). Three to six microliters of the resulting giant liposome suspension was deposited onto  $3.5\text{ cm}$  Petri dishes and mixed with  $2\text{ mL}$  of  $10\text{ mM}$  Mes buffer, pH 4, containing  $100\text{ mM}$  KCl for electrical recording (bath solution). Patch electrodes were filled with a solution containing  $10\text{ mM}$  Hepes buffer, pH 7, and  $100\text{ mM}$  KCl (pipet solution). Giga seals were formed on giant liposomes with microelectrodes of  $7\text{--}10\text{ M}\Omega$  open resistance. Standard inside-out patch-clamp recordings (29) were performed using an Axopatch 200A (Axon Instruments) at a gain of  $50\text{ mV/pA}$ . Recordings were filtered at  $1\text{ kHz}$  with an 8-pole Bessel filter (Frequency Devices). The holding potential was applied to the interior of the patch pipet, and the bath was maintained at virtual ground. An Ag-AgCl wire was used as the reference electrode through an agar bridge. The data were analyzed with pClamp9 software (Axon Instruments). All measurements were made at room temperature.

## RESULTS

**In Vitro KcsA Unfolding.** The tetrameric potassium channel KcsA contains five tryptophan residues per subunit, which are located either at the ends of the two transmembrane segments (W26, W87, and W113) or at the pore region that

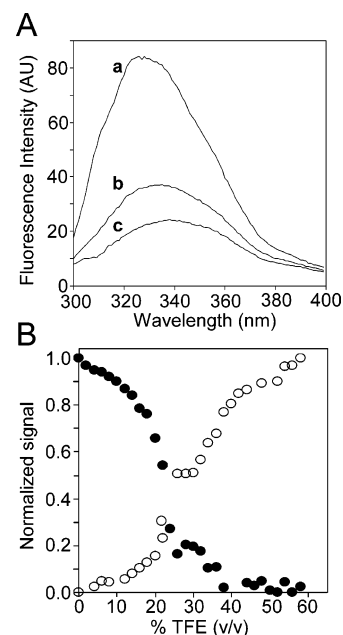


FIGURE 1: TFE-induced fluorescence changes in KcsA. (A) Fluorescence emission spectra of wild-type KcsA in the absence (a) and in the presence of 30% (v/v) (b) and 40% (v/v) (c) TFE. (B) Changes in the normalized values of the fluorescence intensity at 340 nm (closed circles) and the averaged emission intensity (open circles) in the 0–60% (v/v) TFE concentration range. For the experiments shown in the figure, the final KcsA concentration was  $0.2\text{ }\mu\text{M}$  and the buffer was  $20\text{ mM}$  Hepes, pH 7.0, and  $100\text{ mM}$  KCl containing  $5\text{ mM}$  DDM. The excitation wavelength was  $280\text{ nm}$ . Unless indicated otherwise, here and in all other figures the experiments were carried out at  $25\text{ }^\circ\text{C}$ .

connects them (W67 and W68). The spectra of the intrinsic fluorescence emitted by both wild-type 1–160 KcsA and the chymotryptic 1–125 KcsA, solubilized in buffer containing the detergent DDM, are superimposable and show maxima at  $325\text{ nm}$ , suggesting that, in both proteins, most of the tryptophans are located in a hydrophobic environment. In the presence of increasing concentrations of TFE (Figure 1A), a reduction in the fluorescence intensity and a spectral red shift (maxima at  $340\text{ nm}$ ) were similarly observed for the two detergent-solubilized proteins. Monitoring the changes in the fluorescence intensity at  $340\text{ nm}$  of wild-type KcsA (Figure 1B) revealed that a linear decrease in the fluorescence occurs first, starting at the lowest concentrations of TFE in the titration curves. Such a linear decrease in the protein intrinsic fluorescence at low TFE concentration is similar to that seen when a free tryptophan derivative, tryptophan octyl ester (30), in DDM solution, is used for the TFE titrations (data not shown), thus suggesting that in KcsA some of the tryptophan residues are readily accessible to the solvent even at these low TFE concentrations. The initial linear decrease in fluorescence is followed by a sigmoidal-like loss of the fluorescence signal (Figure 1B) which, depending upon the protein concentration (see below), occurs at characteristic midpoint concentrations of TFE [ $22\text{--}24\%$  TFE (v/v) for the conditions used in Figure 1]. Finally, at concentrations of TFE even higher, a second sigmoid-like loss in fluorescence intensity is observed. This latter process occurs at characteristic midpoint concentrations of TFE which were also dependent upon the protein concentration [ $33\text{--}37\%$  TFE (v/v) for the conditions used in Figure 1]. The above results suggest that as the TFE concentration is increased, there are

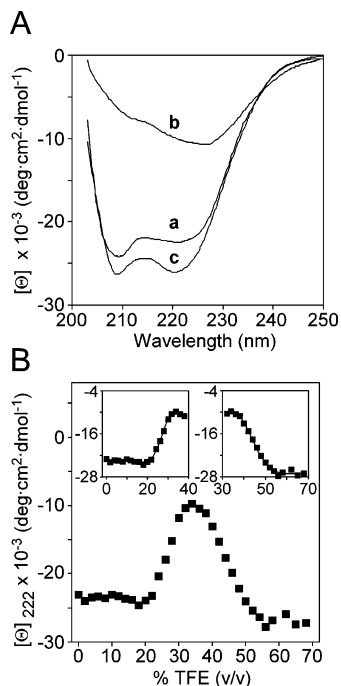


FIGURE 2: CD monitoring of the TFE effect on KcsA. (A) Far-UV circular dichroism spectra of wild-type KcsA in the absence (a) and in the presence of 35% (v/v) (b) and 65% (v/v) (c) TFE. (B) TFE concentration-dependent changes in the molar ellipticity at 222 nm of KcsA in the 0–70% TFE (v/v) concentration range. The insets show the sigmoidal fittings of the two cooperative transitions observed. For simplicity, the transitions were considered as not overlapping. The error introduced by this approximation does not affect the overall conclusions. In the experiments chosen for this figure, the KcsA concentration was 5  $\mu$ M and the buffer was as indicated in the legend of Figure 1.

two subsequent cooperative structural rearrangements in which different populations of previously buried tryptophan residues become exposed to the solvent. Similar observations regarding the occurrence of the two cooperative processes from above were also made by monitoring the spectral red shift in terms of the averaged emission intensity (Figure 1B). Also, no significant differences were found in these experiments when 1–125 KcsA was used instead of wild-type KcsA (data not shown).

The effects of TFE on wild-type KcsA and 1–125 KcsA were also studied by following the far-UV CD spectra at different TFE concentrations (Figure 2A). Again, essentially identical results were obtained with the two proteins which, in the absence of TFE and as expected from the structural information available (11, 12), exhibited CD spectra characteristic of a predominantly  $\alpha$ -helical secondary structure with minima at 208 and 222 nm. Thus, we followed the changes in the molar ellipticity at 222 nm to illustrate the effects of increasing concentrations of TFE on the CD spectra (Figure 2B). It should be noticed that the presence of increasing TFE in these experiments does not result in significant changes in the absorbance of the protein samples. This precludes a major scattering contribution to the observed CD spectra. Similarly to the fluorescence results from above, a biphasic behavior was observed. The first phase consisted of a progressive loss of  $\alpha$ -helical features in which the molar ellipticity at 222 nm increases up to a maximum (spectrum depicted as “b” in Figure 2A) in a sigmoid-like manner. For any given protein concentration, the midpoint TFE concen-

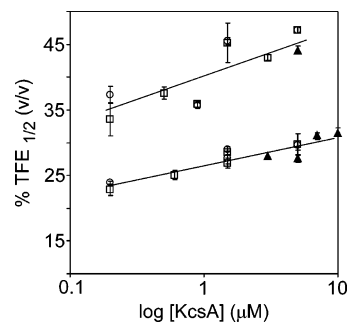


FIGURE 3: KcsA concentration dependence of the TFE concentration midpoints obtained from sigmoidal fitting of the two TFE-induced cooperative transitions illustrated in Figures 1B and 2B. Data from the fluorescence red shift observed in the averaged emission intensity (open circles) and from the changes in the fluorescence emission intensity (open squares), as well as in the molar ellipticity at 222 nm from the CD spectra (closed triangles), are shown. Lines are mere guides to the eye.

tration corresponding to such sigmoidal process [27% TFE (v/v) for the conditions used in Figure 2] was practically identical to that determined by fluorescence for the first cooperative transition described above, thus suggesting that tryptophan exposure to the solvent caused by increasing TFE is accompanied by a loss of  $\alpha$ -helical secondary structure. Similar effects of TFE in inducing the unfolding of different proteins have been reported elsewhere (31–33).

Use of even higher TFE concentrations in the CD titration experiments revealed that a second sigmoid-like transition occurs with a TFE concentration midpoint of approximately 45% (v/v) for the conditions shown in Figure 2. Here, a decrease rather than an increase in the molar ellipticity at 222 nm is observed, which indeed goes beyond the initial value exhibited by the native protein (spectrum “c” in Figure 2A). This is consistent with the well-known induction of helical structure by high concentrations of TFE, which has been reported for many proteins and peptides (34, 35). Nevertheless, the adoption of a given structure under these conditions of high concentrations of TFE is not straightforward and seems to be strongly dependent on protein concentration. For example, the amide I’ band in Fourier transform infrared spectra (FTIR) of samples at similarly high TFE concentrations, but taken at approximately 0.65 mM KcsA (within the usual range of protein concentrations used in FTIR, but much higher than those used in the fluorescence and CD experiments), shows a maximum at 1645  $\text{cm}^{-1}$ , indicative of the predominance of nonordered protein structures. Moreover, heating of these samples in the FTIR sample cell results in the appearance of absorbance bands at 1686 and 1620  $\text{cm}^{-1}$  (characteristic of intermolecular protein aggregates) which do not appear in the absence of TFE except at very high temperatures (not shown).

Within the 0.2–10.0  $\mu$ M KcsA concentration range used here, the above CD and fluorescence experiments reveal a protein concentration dependence (Figure 3), which is to be expected both for the unfolding of oligomeric proteins (36, 37) and for an intermolecular protein aggregation process. Figure 3 also shows that, for the same protein concentrations, the values of the TFE midpoints for the two cooperative transitions do not depend on whether CD or fluorescence monitoring is used in the experiments.

*Micellar Disruption by TFE.* Previous studies on protein-free DDM micelles in TFE–water mixtures revealed that

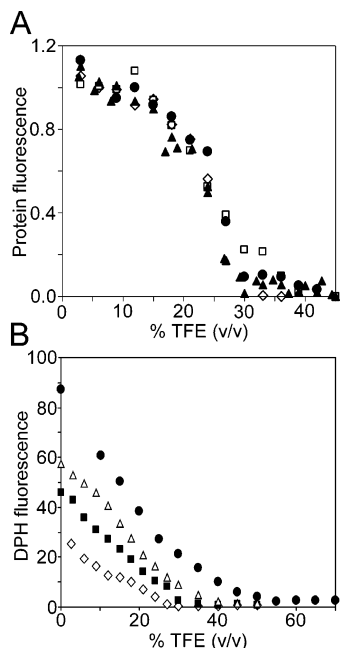


FIGURE 4: TFE-induced protein changes vs micellar disruption. (A) Changes in the normalized values of the KcsA fluorescence intensity at 340 nm in the presence of increasing TFE and at different concentrations of DDM: 1 mM (open squares), 10 mM (closed circles), 25 mM (closed triangles), and 50 mM (open diamonds). The KcsA concentration was 2  $\mu$ M. (B) TFE-induced micellar disruption as monitored by the changes in the fluorescence emission at 430 nm of 2.5  $\mu$ M DPH. The excitation wavelength was 360 nm. All samples were prepared at an identical KcsA concentration of 0.2  $\mu$ M in 20 mM Hepes buffer, pH 7.0, and 100 mM KCl containing 5 (open diamonds), 10 (closed squares), 20 (open triangles), or 62 (closed circles) mM DDM.

TFE stabilizes the detergent as a monomer in the aqueous solution by increasing its critical micellar concentration as the TFE concentration increases (data not shown). Therefore, there is the possibility that rather than reporting exclusively on a true TFE-induced protein structural rearrangement our results from above might partly be reflecting the exposure of the protein to the aqueous environment upon micellar disruption by TFE. To check this possibility, additional TFE titration experiments were carried out at a fixed concentration of KcsA and at different DDM concentrations. Figure 4A shows that, regardless of the DDM concentration used in these experiments, the observed midpoints for the TFE-induced cooperative protein unfolding processes remain unaltered. Conversely, micellar disruption caused by increasing TFE was found to be strongly dependent on the detergent concentration (Figure 4B). For these latter experiments we also used samples containing a constant concentration of KcsA and different DDM concentrations and DPH as a probe (38). DPH was chosen for these experiments because it is highly fluorescent in hydrophobic environments, such as that provided by the mixed detergent micelles, whereas it is weakly fluorescent in aqueous media. Serial additions of TFE to a sample containing DPH incorporated into the KcsA–DDM mixed micelles (Figure 4B) caused a steep linear decrease in the fluorescence intensity of the probe, until it reached a point with minimum fluorescence. The fluorescence decrease monitors micellar breakdown, while the first point with the minimum fluorescence indicates the minimum TFE concentration necessary

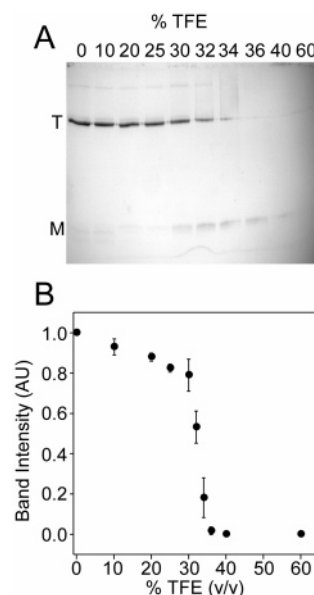


FIGURE 5: SDS–PAGE analysis of the dissociation of wild-type KcsA into its constituent subunits by increasing concentrations of TFE. KcsA samples, at a protein concentration of 3  $\mu$ M, in 20 mM Hepes buffer, pH 7.0, and 100 mM KCl containing 5 mM DDM were treated with TFE during 30 min to the final TFE concentrations (v/v) given in the figure, then mixed 1:1 (by volume) with electrophoresis sample buffer (20 mM Tris, pH 6.0, containing 20% glycerol, 4% SDS, and 0.1% bromophenol blue), and deposited into the wells of an 13.5% acrylamide gel. Panel A shows a representative Coomassie Blue stained gel in which the tetrameric (T) and monomeric (M) forms of KcsA are indicated. Panel B shows the results (mean and standard deviation) obtained from densitometric analysis of several gels on the disappearance of the tetrameric KcsA species.

to totally disrupt the micelles at each of the detergent concentrations used in the studies. Therefore, we concluded that the sigmoidal transitions obtained in the KcsA intrinsic fluorescence and CD experiments from above truly report on cooperative protein structural rearrangements induced by TFE, which are not a direct consequence of micellar disruption.

**Dissociation of KcsA into Its Constituent Subunits.** KcsA has been shown to be remarkably stable in SDS and to migrate mostly as a homotetramer in SDS–PAGE gels as long as the samples for electrophoresis are not heated at high temperatures (17, 20, 39). Thus, SDS–PAGE provides a simple means to study the effects of destabilizing agents such as TFE on the oligomerization state of KcsA (Figure 5A). It should be noticed that the presence of TFE in the electrophoretic samples causes the lower molecular weight sample components to appear as faint bands in the gel or to not appear at all (19), and under these conditions, only the disappearance of the KcsA tetramer rather than monomer appearance could be reliably measured by densitometry (Figure 5B). Nonetheless, as reported by others (19) and also in our own experience, the presence of the monomer under these conditions can be evidenced by eliminating the TFE from the samples prior to gel electrophoresis.

The SDS–PAGE results indicate that TFE, at concentrations apparently higher than that corresponding to the first cooperative unfolding process observed in the fluorescence and CD measurements from above, causes the dissociation of the tetrameric KcsA. Again, results very similar to those shown on Figure 5 were obtained when 1–125 KcsA was

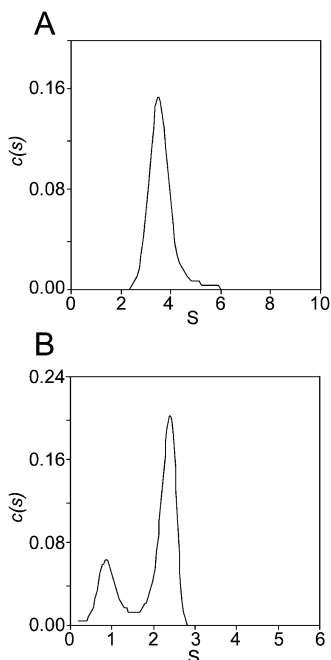


FIGURE 6: Differential sedimentation coefficient distributions of KcsA in the presence of TFE. Illustrative sedimentation coefficient profiles derived from sedimentation velocity experiments carried out with KcsA in the presence of 12% (panel A) and 24% (panel B) TFE (v/v). After correction for the viscosity and density of the different TFE solutions,  $s_{20,w}$  values for the different populations shown in the figure were 5.4 S (panel A) and 2.0 and 5.9 S (panel B). The KcsA concentration was 5  $\mu$ M. The temperature was 21  $^{\circ}$ C.

used instead of wild-type KcsA, except that the molecular weights of the tetramer and the monomer in the proteolyzed 1–125 KcsA were those expected from the chymotrypsin cleavage (not shown). Nonetheless, there are many reasons why the SDS–PAGE results cannot be strictly compared to those from the fluorescence and CD measurements. For instance, the electrophoresis analysis introduces an important additional component in the media (the detergent SDS), which is not present in the spectroscopic measurements. Also, dilution of the TFE concentration with electrophoresis sample buffer of the TFE-treated samples might cause the “effective” TFE concentrations to be indeed overestimated, particularly when the dissociation process is partly reversible, as happens to be the case here (see below). Because of these and other limitations, additional analytical ultracentrifugation experiments were conducted in which both the media components and the protein concentration were comparable to those used for the fluorescence and CD measurements. Figure 6 shows sedimentation velocity results obtained at different TFE concentrations. For instance, at 12% (v/v) TFE, where KcsA is fully folded (Figure 6A), there is a single sedimenting species which, after correcting for the differences in viscosity and density produced by the presence of TFE, has a sedimentation coefficient which, assuming a spherical shape and a protein partial specific volume of 0.73  $\text{cm}^3/\text{g}$ , corresponds to an apparent molecular mass ranging from 80 to 100 kDa. This fits fairly well to the theoretical molecular mass of 76 kDa for the KcsA tetramer (160 amino acids per monomer for the native protein, plus 12 additional N-terminal amino acids containing the polyhistidine tag) bound to a reasonable number of DDM molecules. At 24% TFE (v/v)

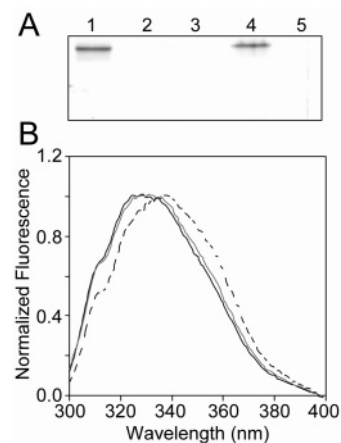
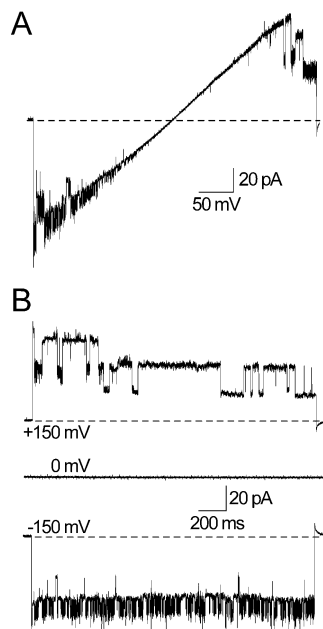


FIGURE 7: Refolding and tetramerization of KcsA. Panel A shows an SDS–PAGE analysis of a typical KcsA refolding experiment at 5  $\mu$ M protein concentration. Lane 1 shows the characteristic tetrameric KcsA that has not been submitted to treatment with TFE. Lanes 2 and 3 show how the tetramer species disappeared completely from identical aliquots of KcsA as a consequence of treatment with TFE at 35% (lane 2) and 50% (lane 3) (v/v). Lanes 4 and 5 result respectively from diluting the samples from lanes 2 and 3 to a final TFE concentration of 10% (v/v). The reappearance of the tetrameric species can be observed in the dilution from the 35% sample (lane 4) but not from the 50% sample (lane 5). Equivalent amounts of the KcsA protein were loaded into each well in the electrophoresis gel. Panel B shows the normalized fluorescence spectra of KcsA at a final protein concentration of 1.5  $\mu$ M in 4% (solid line) and 32% (dashed line) TFE (v/v). The spectrum of the latter sample upon dilution to a final concentration of 4% TFE (v/v) (gray line) is also shown to illustrate the recovery of the fluorescence spectral shape upon refolding.

(Figure 6B), such “tetrameric” species is accompanied by a lighter one, whose corrected sedimentation coefficient yields an apparent molecular mass practically identical to that of the KcsA monomer, 19 kDa. From a series of similar experiments carried out in the presence of increasing concentrations of TFE, the estimated TFE concentration midpoint for the tetramer to monomer conversion was approximately 25% (v/v), which for the protein concentration used in these studies is practically identical to those determined from the fluorescence and CD measurements from above.

*In Vitro Refolding of KcsA.* A previous attempt to refold TFE-unfolded KcsA has been reported (17). In that work, monomeric KcsA prepared by treatment with 50% TFE acidified with 1% trifluoroacetic acid could only be refolded to tetrameric KcsA with a low efficiency (20–30%) and only upon reconstitution into lipids. In our hands, we also found that indeed, at TFE concentrations above the TFE midpoint for the second cooperative event (i.e., higher than 45%; see above), the DDM-solubilized KcsA dissociates irreversibly. Conversely, treatment with TFE at concentrations not exceeding those at which the first cooperative transition is just completed and in which KcsA is both unfolded and dissociated into subunits makes it possible that KcsA can be successfully reassembled into tetramers by simple 3-fold or higher dilution of the TFE denaturant in the usual detergent-containing TFE-free buffer, as seen by SDS–PAGE (Figure 7A). The extent of tetramer recovery was quantified by densitometry of the bands corresponding to tetrameric KcsA, resulting in an approximately 80% yield under these experimental conditions.



**FIGURE 8:** Electrophysiological recordings of the refolded KcsA. Representative patch-clamp recordings in excised membrane patches from reconstituted asolectin giant liposomes prepared from refolded KcsA (treated with 35% TFE at a KcsA concentration of 7  $\mu$ M, then diluted to a final 12.5% TFE concentration, and used for reconstitution). (A) Typical voltage ramp obtained from  $-200$  to  $+200$  mV. (B) Membrane potential pulses at  $+150$ ,  $0$ , and  $-150$  mV. The zero current level at each voltage is indicated by a dotted line.

The refolding process was further followed by comparing the fluorescence spectra of the unfolded and refolded forms of KcsA (Figure 7B). Because the refolded samples are diluted 3–6-fold with respect to the unfolded samples, we use normalized spectra in Figure 7B to facilitate comparison among the different samples. It is observed that the characteristic red shift referred to in Figure 1 for the fluorescence emission spectra of the TFE-unfolded samples is almost completely reversed in the refolded samples, in which the fluorescence spectra are practically undistinguishable from those of native KcsA. Although not shown by the normalized spectra, such a recovery of the spectral shape is accompanied by an increase in the fluorescence intensity, which also goes back to values very similar to those seen in the native protein. This is to conclude that *in vitro* refolding of KcsA tetramers in detergent solution from TFE-unfolded KcsA monomers is indeed a very efficient process.

In an attempt to determine whether the refolded KcsA recovers the characteristic ion channel activity of the native protein, the refolded samples were also reconstituted into giant liposomes made from asolectin lipids to assess potassium channel activity in excised membrane patches by patch-clamp methods. Figure 8 shows that, similarly to the previous report mentioned above (17) on the low efficiency and lipid-requiring refolding of KcsA, the refolded KcsA reconstituted into an artificial membrane shows natively like, potassium channel activity, including frequent events of coupled gating, a characteristic feature of native KcsA when reconstituted into giant liposomes (manuscript in preparation). Furthermore, the probability of finding active versus silent patches in the refolded preparations was similar to that found for the native, untreated protein. Thus, these observations strongly suggest

that KcsA refolding includes the recovery of its biological activity.

## DISCUSSION

Fluorescence and CD monitoring of the effects of increasing concentrations of TFE on the tetrameric potassium channel KcsA shows a first protein concentration-dependent, cooperative transition which, depending on the protein concentration, occurs in the 22–30% (v/v) TFE concentration range and involves an increased exposure of tryptophan residues to the solvent and an important loss of the protein helical structure. Such observations support the notion that a TFE-induced cooperative unfolding of the oligomeric KcsA occurs at those TFE concentrations. Because of the similarity between the TFE concentration midpoints determined by fluorescence and CD measurements, such unfolding seemingly follows a simple, two-state transition under equilibrium conditions, in which the native tetrameric folded protein, N, is converted into a partially unfolded product, U. Subsequently, increasing the TFE concentration even further [35–45% (v/v), depending on the protein concentration] leads to a second cooperative event in which the partly unfolded protein, U, is converted into what we would call a TFE-denatured state, D, which might correspond to either a highly folded final product with an abnormally high helical content, as seen by CD at low protein concentrations, or a nonordered, intermolecular aggregate as seen by FT-IR measurements at high protein concentrations.

It should be noticed that, in parallel to the occurrence of the above protein-related events, there is also disruption of the DDM–protein mixed micelles caused by the stabilization of detergent monomers in solution as the TFE concentration is increased. Depending on the detergent concentration, complete micellar disruption may occur either before or after the production of the unfolded state, U, but in any case it does not affect the observed cooperative protein unfolding, and thus, it could be ignored for the purpose of reporting on the occurrence of protein events.

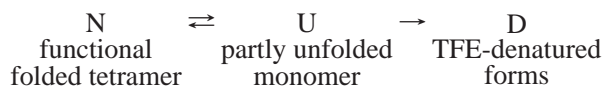
The effects of TFE on the dissociation into subunits of the tetrameric KcsA have been monitored both by SDS–PAGE and by analytical ultracentrifugation. Estimates of the TFE concentration midpoints for the dissociation process as obtained from the SDS–PAGE experiments might be misleading for several reasons. These include the presence of SDS in the media or the dilution of the TFE-treated samples with electrophoresis sample buffer prior to the electrophoresis run. On the other hand, the analytical ultracentrifugation experiments, which are obtained under experimental conditions comparable to those used in the fluorescence and CD monitoring, indicate that, in the absence of SDS, KcsA dissociation occurs at TFE concentrations very similar to those causing the first cooperative transition detected in the above fluorescence and CD studies. Moreover, dissociation of KcsA into subunits under these conditions received additional support from  $^1\text{H}$  1D NMR measurements that showed that different resonance signals from KcsA (15  $\mu$ M) were narrower in the presence of 30% TFE than in its absence (data not shown), as expected for species of lower molecular mass. All of the above data suggest that tetramer dissociation and protein unfolding are linked, coupled processes. Such conclusion seems reminiscent of that found

in a somewhat simpler system, the T1 or prime tetramerization domain of Shaker B, an eukaryotic potassium channel, in which folding and tetramerization are also coupled (40). Finally, the observation of KcsA monomers at the above TFE concentrations supports the assignment of the observed partly unfolded product in solution, U, to a KcsA monomer.

Previous studies of unfolding of KcsA by increasing concentrations of TFE (18, 19) reported that an irreversible dissociation and unfolding of KcsA, followed by SDS-PAGE and CD, respectively, occurred at TFE concentrations significantly lower than those reported here. This apparent discrepancy is mostly due to the fact that those authors used sodium-containing buffers in their measurements, instead of the potassium-containing buffers used in this work. The presence of sodium and/or lack of potassium is known to lead to functional collapse of most potassium channels (41, 42), and indeed, we have found that sodium ions greatly destabilize the structure of KcsA (manuscript in preparation), so that the protein in sodium buffers is much more susceptible to the presence of TFE.

A particularly interesting contribution of this work is that decreasing the TFE concentration by simple dilution from the U, but not from the D state, results in the highly efficient refolding of the protein. Such a refolding process includes the reappearance of the characteristic tetrameric form of KcsA, suggesting that, similarly to the observations on the apparent coupling between KcsA unfolding and dissociation, refolding and tetramerization of KcsA might also be coupled or, at least, occur concomitantly. Moreover, following reconstitution into giant liposomes, the refolded KcsA exhibits nativelike ion channel activity, which means that protein refolding restores also its biological activity.

The simplest scheme to account for all of these observations is given below, where N, U, and D stand for the native, unfolded, and denatured states of the protein, as defined above. Such a scheme would be applicable both to wild-type KcsA and to its proteolytic derivative 1–125 KcsA, both of which yielded practically identical results in these experiments, despite the fact that 1–125 KcsA lacks most of the C-terminal, cytoplasmic domain of the protein.



To the best of our knowledge, this is the first report on a highly efficient *in vitro* refolding and oligomerization from an unfolded and monomeric state of a “bona fide” oligomeric and predominantly helical membrane protein. Nonetheless, it has been mentioned already that a previous attempt to refold KcsA has been published (17) in which the purified protein was treated directly with 50% TFE (v/v) acidified with 1% trifluoroacetic acid. These authors did not use lower TFE concentrations, and under their harsh experimental conditions, refolding of the protein occurs with a low efficiency (20–30%) and only upon reconstitution into lipids as coadjuvants of the process, which led them to conclude that the presence of lipids was a strict requirement for protein refolding (17). Clearly, this is not the case here, as we have shown that use of milder experimental conditions (lower TFE concentrations) leading to the production of the U state does allow for a highly efficient protein refolding and oligomerization (~80% yield) in plain detergent solution, i.e., in the

absence of any added lipids. Furthermore, we also observed that use of high TFE concentrations comparable to those used by Valiyaveetil and co-workers (17) leads to production of the D state, whose refolding is indeed absolutely irreversible in detergent solution. Nonetheless, preliminary evidence from our laboratory indicates that the already high yields of refolding in detergent solution observed in our studies can be increased even further, to virtually 100%, in the presence of specific lipids in the refolding media (manuscript in preparation), leading to the conclusion that lipid–protein interaction is not a strict requirement for the refolding of KcsA, but it definitively has a role in optimizing the process to make it virtually quantitative.

In summary, we have reported that, besides the irreversible denaturation of the protein (the D state) induced by high concentration of TFE, the TFE-induced interconversion between the N and the U states in plain detergent solution seems to obey a simple, highly reversible two-state transition under equilibrium conditions, in which the native tetrameric KcsA protein is converted into partly unfolded monomers and vice versa in such a way that unfolding and dissociation into subunits (in the N to U direction) or refolding and tetramerization (in the U to N direction) are seemingly coupled. The similarities observed in these studies between wild-type and 1–125 KcsA indicate that the 126–160 C-terminal segment of the protein does not play a significant role in these processes. More studies are now in progress to complement these equilibrium observations by exploring the kinetics and thermodynamics of the unfolding and refolding processes.

#### ACKNOWLEDGMENT

We thank Dr. Germán Rivas and Dr. Carlos Alfonso (Centro de Investigaciones Biológicas, CSIC, Madrid) for help with the analytical ultracentrifugation experiments. We also acknowledge Dr. Jesús Sanz and Dr. Javier Gómez from this Institute and Dr. Francico Gavilanes (Universidad Complutense de Madrid) for critical revision of the manuscript and useful suggestions and Mrs. Eva Martínez for excellent technical help throughout.

#### REFERENCES

- Booth, P. J., and Curran, A. R. (1999) Membrane protein folding, *Curr. Opin. Struct. Biol.* 9, 115–121.
- Booth, P. J., Templer, R. H., Meijberg, W., Allen, S. J., Curran, A. R., and Lorch, M. (2001) *In vitro* studies of membrane protein folding, *Crit. Rev. Biochem. Mol. Biol.* 36, 501–603.
- Booth, P. J. (2003) The trials and tribulations of membrane protein folding *in vitro*, *Biochim. Biophys. Acta* 1610, 51–56.
- Tamm, L. K., Hong, H., and Liang, B. (2004) Folding and assembly of beta-barrel membrane proteins, *Biochim. Biophys. Acta* 1666, 250–263.
- Popot, J. L., and Engelman, D. M. (1990) Membrane protein folding and oligomerization: the two-stage model, *Biochemistry* 29, 4031–4037.
- Huang, K. S., Bayley, H., Liao, M. J., London, E., and Khorana, H. G. (1981) Refolding of an integral membrane protein. Denaturation, renaturation, and reconstitution of intact bacteriorhodopsin and two proteolytic fragments, *J. Biol. Chem.* 256, 3802–3809.
- London, E., and Khorana, H. G. (1982) Denaturation and renaturation of bacteriorhodopsin in detergents and lipid-detergent mixtures, *J. Biol. Chem.* 257, 7003–7011.
- Lau, F. W., and Bowie, J. U. (1997) A method for assessing the stability of a membrane protein, *Biochemistry* 36, 5884–5892.

9. Nagy, J. K., Lau, F. W., Bowie, J. U., and Sanders, C. R. (2000) Mapping the oligomeric interface of diacylglycerol kinase by engineered thiol cross-linking: homologous sites in the transmembrane domain, *Biochemistry* 39, 4154–4164.
10. Schrempf, H., Schmidt, O., Kummerlen, R., Hinnah, S., Muller, D., Betzler, M., Steinkamp, T., and Wagner, R. (1995) A prokaryotic potassium ion channel with two predicted transmembrane segments from *Streptomyces lividans*, *EMBO J.* 14, 5170–5178.
11. Doyle, D. A., Morais, C. J., Pfuetzner, R. A., Kuo, A., Gulbis, J. M., Cohen, S. L., Chait, B. T., and MacKinnon, R. (1998) The structure of the potassium channel: molecular basis of K<sup>+</sup> conduction and selectivity, *Science* 280, 69–77.
12. Cortes, D. M., Cuello, L. G., and Perozo, E. (2001) Molecular architecture of full-length KcsA: role of cytoplasmic domains in ion permeation and activation gating, *J. Gen. Physiol.* 117, 165–180.
13. Heginbotham, L., Odessey, E., and Miller, C. (1997) Tetrameric stoichiometry of a prokaryotic K<sup>+</sup> channel, *Biochemistry* 36, 10335–10342.
14. Cuello, L. G., Romero, J. G., Cortes, D. M., and Perozo, E. (1998) pH-dependent gating in the *Streptomyces lividans* K<sup>+</sup> channel, *Biochemistry* 37, 3229–3236.
15. Heginbotham, L., Kolmakova-Partensky, L., and Miller, C. (1998) Functional reconstitution of a prokaryotic K<sup>+</sup> channel, *J. Gen. Physiol.* 111, 741–749.
16. LeMasurier, M., Heginbotham, L., and Miller, C. (2001) KcsA: it's a potassium channel, *J. Gen. Physiol.* 118, 303–314.
17. Valiyaveetil, F. I., Zhou, Y., and MacKinnon, R. (2002) Lipids in the structure, folding, and function of the KcsA K<sup>+</sup> channel, *Biochemistry* 41, 10771–10777.
18. van den Brink-van der Laan, E., Chupin, V., Killian, J. A., and de Kruijff, B. (2004) Small alcohols destabilize the KcsA tetramer via their effect on the membrane lateral pressure, *Biochemistry* 43, 5937–42.
19. van den Brink-van der Laan, E., Chupin, V., Killian, J. A., and de Kruijff, B. (2004) Stability of KcsA tetramer depends on membrane lateral pressure, *Biochemistry* 43, 4240–4250.
20. Molina, M. L., Encinar, J. A., Barrera, F. N., Fernandez-Ballester, G., Riquelme, G., and Gonzalez-Ros, J. M. (2004) Influence of C-terminal protein domains and protein–lipid interactions on tetramerization and stability of the potassium channel KcsA, *Biochemistry* 43, 14924–14931.
21. Pace, C. N., and Scholtz, J. M. (1997) Measuring the conformational stability of a protein, in *Protein Structure: A Practical Approach* (Creighton, T. E., Ed.) IRL Press at Oxford University Press, Oxford.
22. Royer, C. A. (1995) Fluorescence spectroscopy in protein stability and folding, in *Methods in Molecular Biology* (Shirley, B. A., Ed.) Humana Press, Totowa, NJ.
23. Echabe, I., Encinar, J. A., and Arrondo, J. L. R. (1997) Removal of spectral noise in the quantitation of protein structure through infrared band decomposition, *Biospectroscopy* 3, 469–475.
24. Bañuelos, S., Arrondo, J. L., Goni, F. M., and Pifat, G. (1995) Surface-core relationships in human low-density lipoprotein as studied by infrared spectroscopy, *J. Biol. Chem.* 270, 9192–9196.
25. Laemmli, U. K. (1970) Cleavage of structural proteins during the assembly of the head of bacteriophage T4, *Nature* 227, 680–685.
26. Schuck, P. (2000) Size-distribution analysis of macromolecules by sedimentation velocity ultracentrifugation and lamm equation modelling, *Biophys. J.* 78, 1606–1619.
27. Gonzalez, J. M., Velez, M., Jimenez, M., Alfonso, C., Schuck, P., Mingorance, J., Vicente, M., Minton, A. P., and Rivas, G. (2005) Cooperative behavior of *Escherichia coli* cell-division protein FtsZ assembly involves the preferential cyclization of long single-stranded fibrils, *Proc. Natl. Acad. Sci. U.S.A.* 102, 1895–1900.
28. Riquelme, G., Lopez, E., Garcia-Segura, L. M., Ferragut, J. A., and Gonzalez-Ros, J. M. (1990) *Biochemistry* 29, 11215–11222.
29. Hamill, O. P., Marty, A., Neher, E., Sakmann, B., and Sigworth, F. J. (1981) Improved patch-clamp techniques for high-resolution current recording from cells and cell-free membrane patches, *Pfluegers Arch.* 391, 85–100.
30. de Foresta, B., Gallay, J., Sopkova, J., Champeil, P., and Vincent, M. (1999) Tryptophan octyl ester in detergent micelles of dodecylmaltoside: fluorescence properties and quenching by brominated detergent analogs, *Biophys. J.* 77, 3071–3084.
31. Gast, K., Zirwer, D., Muller-Frohne, M., and Damaschun, G. (1999) Trifluoroethanol-induced conformational transitions of proteins: insights gained from the differences between alpha-lactalbumin and ribonuclease A, *Protein Sci.* 8, 625–634.
32. Huang, K., Park, Y. D., Cao, Z. F., and Zhou, H. M. (2001) Reactivation and refolding of rabbit muscle creatine kinase denatured in 2,2,2-trifluoroethanol solutions, *Biochim. Biophys. Acta* 1545, 305–313.
33. Jasanoff, A., and Fersht, A. R. (1994) Quantitative determination of helical propensities from trifluoroethanol titration curves, *Biochemistry* 33, 2129–2135.
34. Kentsis, A., and Sosnick, T. R. (1998) Trifluoroethanol promotes helix formation by destabilizing backbone exposure: desolvation rather than native hydrogen bonding defines the kinetic pathway of dimeric coiled coil folding, *Biochemistry* 37, 14613–14622.
35. Chiti, F., Taddei, N., Webster, P., Hamada, D., Fiaschi, T., Ramponi, G., and Dobson, C. M. (1999) Acceleration of the folding of acylphosphatase by stabilization of local secondary structure, *Nat. Struct. Biol.* 6, 380–387.
36. Mateu, M. G. (2002) Conformational stability of dimeric and monomeric forms of the C-terminal domain of human immunodeficiency virus-1 capsid protein, *J. Mol. Biol.* 318, 519–531.
37. Jaenicke, R., and Lilie, H. (2000) Folding and association of oligomeric and multimeric proteins, *Adv. Protein Chem.* 53, 329–401.
38. Chattopadhyay, A., and London, E. (1984) Fluorimetric determination of critical micelle concentration avoiding interference from detergent charge, *Anal. Biochem.* 139, 408–412.
39. Cortes, D. M., and Perozo, E. (1997) Structural dynamics of the *Streptomyces lividans* K<sup>+</sup> channel (SKC1): oligomeric stoichiometry and stability, *Biochemistry* 36, 10343–10352.
40. Robinson, J. M., and Deutsch, C. (2005) Coupled tertiary folding and oligomerization of the T1 domain of Kv channels, *Neuron* 45, 223–232.
41. Gomez-Lagunas, F., Batista, C. V., Olamendi-Portugal, T., Ramirez-Dominguez, M. E., and Possani, L. D. (2004) Inhibition of the collapse of the Shaker K<sup>+</sup> conductance by specific scorpion toxins, *J. Gen. Physiol.* 123, 265–279.
42. Loboda, A., Melishchuk, A., and Armstrong, C. (2001) Dilated and defunct K channels in the absence of K<sup>+</sup>, *Biophys. J.* 80, 2704–2714.

BI050845T